

Ultraviolet Photoelectron Spectroscopy of the *o*-, *m*-, and *p*-Benzyne Negative Ions. Electron Affinities and Singlet–Triplet Splittings for *o*-, *m*-, and *p*-Benzyne

Paul G. Wenthold,^{*,§} Robert R. Squires,^{*,‡} and W. C. Lineberger^{*,†}

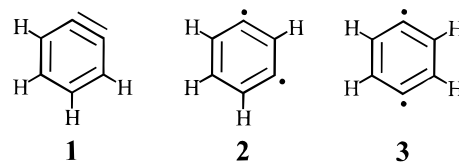
Contribution from the Department of Chemistry and Biochemistry, Texas Tech University, Lubbock, Texas 79409-1061, JILA, University of Colorado and National Institute of Standards and Technology, and Department of Chemistry and Biochemistry, University of Colorado, Boulder, Colorado 80309-0440, and Department of Chemistry, Purdue University, West Lafayette, Indiana 47907

Received January 29, 1998

Abstract: The 351 nm photoelectron spectra of the negative ions of *o*-, *m*-, and *p*-benzyne (1,2-, 1,3-, and 1,4-dehydrobenzene, respectively) and their perdeuterated isotopomers have been obtained. The *o*-benzyne ions were generated by the reaction of benzene and benzene-*d*₆ with O⁻, while the *m*- and *p*-benzyne ions were prepared by the gas-phase reaction between the corresponding 3- and 4-(trimethylsilyl)phenyl anions and molecular fluorine, F₂. The photoelectron spectra of the benzyne anions each contain two features, corresponding to formation of the singlet and triplet states of the biradicals. The electron affinities of *o*- and *p*-benzyne are found to be 0.564 ± 0.007 and 1.265 ± 0.008 eV, respectively, while the electron affinities of deuterated *o*- and *p*-benzyne are found to be 8 and 5 meV lower, respectively. The electron affinity of *m*-benzyne could not be determined from the photoelectron spectrum because the origin peak could not be assigned unequivocally. For *o*- and *p*-benzyne, the singlet–triplet energy splittings can be obtained directly from the photoelectron spectrum, with values of 37.5 ± 0.3 and 3.8 ± 0.5 kcal/mol, respectively, obtained for the *h*₄ species and 37.6 ± 0.3 and 3.9 ± 0.5 kcal/mol, respectively, obtained for the fully deuterated molecules. Using a previously reported value for the electron affinity of *m*-benzyne, the singlet–triplet splitting for this molecule is found to be 21.0 ± 0.3 kcal/mol. Vibrational frequencies are reported for the deuterated and nondeuterated forms of all three biradicals and for the corresponding negative ions. Using the measured electron affinities and previously reported heats of formation of *o*-, *m*-, and *p*-benzyne, the gas-phase acidities of the *ortho*, *meta*, and *para* positions of phenyl radical are calculated to be 377.4 ± 3.4, 386.8 ± 3.2, and 393.1 ± 3.0 kcal/mol, respectively, and the C–H bond energies at the *ortho*, *meta*, and *para* positions of phenyl anion are found to be 89.3 ± 3.3, 98.7 ± 3.1, and 105.0 ± 2.9 kcal/mol, respectively. The heats of formation of the singlet and triplet states of the benzyne are found to be in excellent agreement with the predictions derived from simple valence promotion energy models.

Of the many different classes of organic biradicals, the benzyne have accumulated the longest history and most extensive record of experimental and theoretical investigation.¹ Although “1,2-didehydrobenzenes” had been postulated as early as 1870² as intermediates in various reactions, it was the classic work of Wittig³ and Roberts⁴ in the 1940s and 1950s that firmly established the existence of *o*-benzyne **1** as a reactive intermediate in base-induced elimination reactions of halobenzenes. Since then, numerous methods for generating *o*-benzyne have been developed, such that these molecules have now become familiar reagents in organic and organometallic synthesis procedures.^{5–7}

The other two benzyne isomers, *m*-benzyne **2**, and *p*-benzyne **3**, have been more elusive. The flash photolysis experiments



with 1,3- and 1,4-benzenediazonium carboxylates by Berry and co-workers^{8,9} and the mass spectrometric studies of diiodobenzenes by Fisher and Lossing¹⁰ provided some of the earliest evidence for these species. Attempts to generate **2** and **3** by base-induced elimination reactions were reported in the mid-1970s;^{11,12} however, the nature of the intermediates formed in these reactions remained unclear. In 1972 Jones and Bergman¹³ demonstrated the intermediacy of *p*-benzyne in the pyrolysis

[†] University of Colorado.

[‡] Purdue University.

[§] Texas Tech University.

(1) Hoffman, R. W. *Dehydrobenzene and Cycloalkynes*; Academic Press: New York, 1967.

(2) Dreher, E.; Otto, R. *Leibigs Ann. Chem.* **1870**, 154, 93.

(3) Wittig, G. *Naturwiss* **1942**, 30, 696.

(4) Roberts, J. D.; Simmons, H. E.; Carlsmith, L. A.; Vaughan, C. W. *J. Am. Chem. Soc.* **1953**, 75, 3290.

(5) Kauffman, T.; Wirthwein, R. *Angew. Chem., Int. Ed. Engl.* **1971**, 10, 20.

(6) Bryce, M. R.; Vernon, J. M. *Adv. Heterocycl. Chem.* **1981**, 28, 183.

(7) Bennett, M. A.; Schwemlein, H. P. *Angew. Chem., Int. Ed. Engl.* **1989**, 28, 1296.

(8) Berry, R. S.; Clardy, J.; Schafer, M. E. *Tetrahedron Lett.* **1965**, 6, 1003.

(9) Berry, R. S.; Clardy, J.; Schafer, M. E. *Tetrahedron Lett.* **1965**, 6, 1011.

(10) Fischer, I. P.; Lossing, F. P. *J. Am. Chem. Soc.* **1963**, 85, 1018.

(11) Washburn, W. N.; Zahler, R.; Chen, I. *J. Am. Chem. Soc.* **1978**, 100, 5863.

of *cis*-3-hexen-1,5-diyne through isotope-labeling and chemical trapping experiments. Cycloaromatization reactions of enediynes to *p*-benzynes, now known as "Bergman cyclizations",¹⁴ have become an important current focus of anticancer drug design.¹⁵ This is due to the discovery of the endiyne antibiotics—potent antitumor agents that are believed to produce *p*-benzyne-type intermediates in the course of double-stranded DNA cleavage.^{16–18}

Recent experimental work on the benzynes has produced a wealth of new physical data. Various gas-phase thermochemical properties of the benzynes have been determined, including absolute heats of formation,^{19–26} ionization potentials,²⁷ electron affinities,²⁸ and acidities.²⁹ The infrared spectrum of **1** isolated in low-temperature matrixes has been measured by several groups,^{30–35} and the NMR properties³⁶ of *o*-benzyne "guest" trapped in a hemicarcerand "host" have been reported. Recently, Sander and co-workers generated *m*- and *p*-benzyne, **2** and **3**, in argon matrixes by flash photolysis and measured their infrared spectra.^{37,38}

Electronic structure calculations have played an important role in the evolving benzyne story.^{39,40} During the last three decades, more than 30 theoretical studies of the benzynes have been published, with half of these appearing in the last 10 years. Virtually every style of ab initio MO, semiempirical MO, and density functional calculation has been used to investigate the geometries, electronic structures, energetics, and spectroscopic properties of the benzynes. The consensus from high-level calculations is that all three benzynes have singlet ground states

(12) Billups, W. E.; Buynak, J. D.; Butler, D. *J. Org. Chem.* **1979**, *44*, 4218.

(13) Jones, R. R.; Bergman, R. G. *J. Am. Chem. Soc.* **1972**, *94*, 660.

(14) Bergman, R. G. *Acc. Chem. Res.* **1973**, *6*, 25.

(15) *Endiyne Antibiotics as Antitumor Agents*; Borders, D.; Doyle, T. W., Eds.; Marcel Dekker: New York, 1995.

(16) Zein, N.; Sinha, A. M.; McGahren, W. J.; Ellestad, G. A. *Science* **1988**, *240*, 1198.

(17) Nicolau, K. C.; Dai, W.-M. *Angew. Chem., Int. Ed., Engl.* **1991**, *30*, 1387.

(18) Nicolau, K. C.; Smith, A. L. *Acc. Chem. Res.* **1992**, *25*, 497.

(19) Rosenstock, H. M.; Stockbauer, R.; Parr, A. C. *J. Chim. Phys.* **1980**, *77*, 745.

(20) Pollack, S. K.; Hehre, W. J. *Tetrahedron Lett.* **1980**, *21*, 2483.

(21) Maccoll, A.; Mathur, D. *Org. Mass Spectrom.* **1981**, *16*, 261.

(22) Moini, M.; Leroi, G. E. *J. Phys. Chem.* **1986**, *90*, 4002.

(23) Riveros, J. M.; Ingemann, S.; Nibbering, N. M. M. *J. Am. Chem. Soc.* **1991**, *113*, 1053.

(24) Guo, Y.; Grabowski, J. J. *J. Am. Chem. Soc.* **1991**, *113*, 5923.

(25) Wenthold, P. G.; Squires, R. R. *J. Am. Chem. Soc.* **1994**, *116*, 6401.

(26) Matimba, H. E. K.; Crabbendam, A. M.; Ingemann, S.; Nibbering, N. M. M. *J. Chem. Soc., Chem. Commun.* **1991**, 644.

(27) Zhang, X.; Chen, P. *J. Am. Chem. Soc.* **1992**, *114*, 3147.

(28) Wenthold, P. G.; Hu, J.; Squires, R. R. *J. Am. Chem. Soc.* **1996**, *118*, 11865.

(29) Gronert, S.; DePuy, C. H. *J. Am. Chem. Soc.* **1989**, *111*, 9253.

(30) Chapman, O. L.; Mattes, K.; McIntosh, C. L.; Pecansky, J.; Calder, G. V.; Orr, G. *J. Am. Chem. Soc.* **1973**, *95*, 6134.

(31) Chapman, O. L.; Chang, C.-C.; Kolc, J.; Rosenquist, N. R.; Tomioka, H. *J. Am. Chem. Soc.* **1975**, *97*, 6586.

(32) Dunkin, I. R.; MacDonald, J. G. *J. Chem. Soc., Chem. Commun.* **1979**, 772.

(33) Nam, H.-H.; Leroi, G. E. *J. Mol. Struct.* **1987**, *157*, 301.

(34) Wentrup, C.; Blanch, R.; Briehl, H.; Gross, G. *J. Am. Chem. Soc.* **1988**, *110*, 1874.

(35) Radziszewski, J. G.; Hess, B. A., Jr.; Zahradnik, R. *J. Am. Chem. Soc.* **1992**, *114*, 52.

(36) Warmuth, R. *Angew. Chem., Int. Ed. Engl.* **1997**, *36*, 1347.

(37) Marquardt, R.; Sander, W.; Kraka, E. *Angew. Chem., Int. Ed. Engl.* **1996**, *35*, 746.

(38) Marquardt, R.; Balster, A.; Sander, W.; Kraka, E.; Cremer, D.; Radziszewski, J. G. *Angew. Chem. Int. Ed. Engl.* **1998**, *37*, 955.

(39) A listing of the theoretical studies of the benzynes is given by Nash and Squires: Nash, J. J.; Squires, R. R. *J. Am. Chem. Soc.* **1996**, *118*, 11872.

(40) Cramer, C. J.; Nash, J. J.; Squires, R. R. *Chem. Phys. Lett.* **1997**, *277*, 311.

and that **1** is the most stable benzyne isomer while **3** is the least stable isomer. These conclusions are consistent with indirect evidence derived from chemical trapping experiments⁴¹ and with the measured heats of formation for the three benzynes.²⁵

A key property of the benzynes, one that provides an essential link between their thermochemistry, reactivity, and electronic structures, is the energy difference between the singlet ground state and the lowest-lying triplet state, i.e., the "singlet–triplet gap", ΔE_{ST} . The magnitude of ΔE_{ST} for singlet biradicals provides a direct measure of the extent of interaction between the nominally nonbonding orbitals. This, in turn, gives valuable insights regarding the balance of through-bond and through-space components of the interaction.^{42,43} Simple valence-bond models have been proposed by Chen and co-workers that equate the singlet–triplet gaps for singlet biradicals with the reduction in their heats of formation compared to bond energy additivity estimates²⁷ and with the increase in the activation energies for H-atom abstraction reactions relative to monoradicals.^{44,45}

While accurate singlet–triplet splittings are essential for understanding biradicals, they are difficult to measure, and, for some systems, they can be extremely hard to calculate accurately by ab initio methods.^{40,46} One of the best experimental methods for determining singlet–triplet splittings in biradicals, carbenes, and other open-shell organic species is negative ion photoelectron spectroscopy (NIPES).⁴⁷ In this experiment, the output of a UV or visible laser is crossed with a mass-selected beam of negative ions corresponding to the biradical or carbene of interest, and the energy spectrum of the resulting photoelectrons is measured. The adiabatic electron affinity, electronic state term energies, and vibrational frequencies for the neutral photoproduct can be derived from the energy differences between assigned features in the spectrum. The 488 nm photoelectron spectrum of the negative ion of *o*-benzyne, **1**[−], was reported more than 10 years ago by Leopold, Stevens-Miller, and Lineberger (LSL).⁴⁸ Photodetachment to two different electronic states was apparent from the spectrum, and careful assignment of the two electronic band origins provided values for the electron affinity (EA) and ΔE_{ST} of *o*-benzyne of 0.560 ± 0.010 eV and 37.7 ± 0.6 kcal/mol, respectively. Analysis of the vibrational structure in the singlet feature also helped resolve the long-standing controversy regarding the C≡C stretching frequency in *o*-benzyne. The value obtained, 1860 cm^{−1}, was much lower than those derived from low-temperature matrix IR experiments but was in good agreement with theoretical predictions. The most recent measurement of the matrix IR spectrum of *o*-benzyne by Radziszewski and co-workers³⁵ gives a C≡C stretching frequency that is in good agreement with the NIPES results of LSL.

One of the greatest challenges in obtaining photoelectron spectra for negative ions of systems such as the benzynes is the synthesis of the gaseous negative ions. In the LSL study, *o*-benzyne negative ion, **1**[−], was generated by the reaction of benzene with O[−] (eq 1). Deuterium labeling experiments

(41) Lockhart, T. P.; Bergman, R. G. *J. Am. Chem. Soc.* **1981**, *103*, 4091.

(42) Hoffman, R.; Imamura, A.; Hehre, W. J. *J. Am. Chem. Soc.* **1968**, *90*, 1499.

(43) Hoffman, R. *Acc. Chem. Res.* **1971**, *4*, 1.

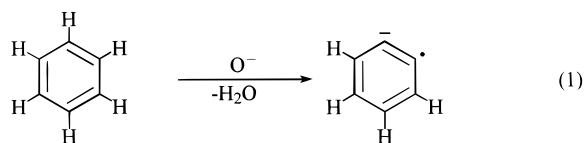
(44) Logan, C. F.; Chen, P. *J. Am. Chem. Soc.* **1996**, *118*, 2113.

(45) Schottelius, M. J.; Chen, P. *J. Am. Chem. Soc.* **1996**, *118*, 4896.

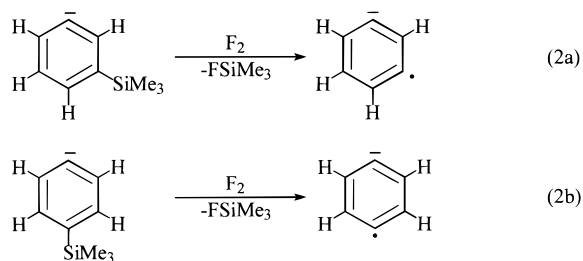
(46) Wierschke, S. G.; Nash, J. J.; Squires, R. R. *J. Am. Chem. Soc.* **1993**, *115*, 11958.

(47) Ervin, K. M.; Lineberger, W. C. In *Advances in Gas-Phase Ion Chemistry*; Adams, N. G.; Babcock, L. M., Eds.; JAI Press: Greenwich, 1992; Vol. 1; p 121.

(48) Leopold, D. G.; Stevens-Miller, A. E.; Lineberger, W. C. *J. Am. Chem. Soc.* **1986**, *108*, 1379.



showed that the reaction proceeds almost entirely by 1,2-abstraction of H_2^+ to produce *o*-benzyne negative ion,⁴⁹ which means that this synthetic approach is not applicable to the formation of the *m*- and *p*-benzyne ion isomers, 2^- and 3^- , respectively. Generation of these ions requires a “regioselective” synthetic procedure in which the 1,3- and 1,4-relationships between the two dehydrocarbons in the radical ions are predefined by the precursors. Recently, Wenthold, Hu, and Squires reported that 2^- and 3^- can be generated in the gas phase as distinct, noninterconverting species by a sequence of reactions resulting in double-desilylation of 1,3- and 1,4-bis-(trimethylsilyl)benzene, respectively (eq 2).^{28,50} Reactions of



these neutral precursors with F^- (or dissociative electron impact ionization) produces the 2- and 3-(trimethylsilyl)phenyl anions. Subsequent reactions of these ions with molecular fluorine, F_2 , yields the isomeric benzyne negative ions by a mechanism that has been described previously.²⁸ Reactivity studies⁵¹ and derivatization²⁸ experiments carried out with these two ions, and with the *ortho* isomer prepared according to eq 1, clearly identified and distinguished the three isomeric structures.

In this paper we report we report the 351 nm photoelectron spectra for *o*-, *m*-, and *p*-benzyne negative ions. The electron affinities and singlet–triplet splittings for *o*-, *m*-, and *p*-benzyne have been determined from detailed analyses of the spectra. Vibronic structure is observed in the singlet and triplet bands of each biradical, from which vibrational frequencies for the benzyne and their negative ions have been derived. The singlet–triplet splittings obtained in the present study have been combined with the measured heats of formation of **1**, **2**, and **3** in order to derive a complete experimental picture of benzyne thermochemistry for comparison with bond energy additivity models, and with results from recent *ab initio* calculations.

Experimental Section

The photoelectron spectrometer and experimental procedures have been described in detail previously,⁴⁷ and only a summary is provided here. Ions are generated in the flowing afterglow source for the photoelectron spectrometer by two methods: (1) by adding a gaseous mixture of the neutral precursor and helium (0.5 Torr) into the plasma produced by a microwave discharge or (2) by ion/molecule reactions between primary ions and neutral reagents gases added through ring inlets downstream in the flow tube. For the present work, the O^- used for the preparation of **1**⁻ was generated by adding O_2 to the microwave discharge. Ions 2^- and 3^- were prepared by adding vapors of the

corresponding bis(trimethylsilyl)benzene just downstream from the discharge, with F_2 (5% in He) added slightly farther downstream. Under these conditions, the 2- and 3-(trimethylsilyl)phenyl anions (eq 2) may be formed either by plasma ionization or by reactions of the bis-(trimethylsilyl)benzenes with F^- present in the reactor;²⁸ these ions then react with fluorine to produce 2^- and 3^- . A small portion of the ions, thermalized to room temperature in the flowing afterglow, are extracted through a 1 mm orifice in a nosecone into a differentially pumped chamber, where they are focused, accelerated to 735 eV, mass selected with a Wien velocity filter ($M/\Delta M \approx 40$), and then decelerated to 40 eV prior to entering the laser interaction region. The ion beam is crossed with the 351 nm output of an argon ion laser in a build-up cavity as described previously.⁴⁷ Photodetached electrons are energy analyzed with ca. 8 meV resolution by a hemispherical analyzer and detected using position-sensitive detection. The photoelectron spectrum depicts the number of electrons detected as a function of electron binding energy, which is given by the difference between the laser photon energy (3.531 19 eV) and the electron kinetic energy.

The absolute energy scale is calibrated by the position of the $^3\text{P}_2 + \text{e}^- \leftarrow ^2\text{P}_{3/2}$ peak in the spectrum of O^- ($\text{EA}(\text{O}) = 1.461\ 12\ \text{eV}$).⁵² A small energy scale compression factor is determined by comparing the measured relative peak positions in the spectrum of tungsten ion with the known term energies of tungsten atom.⁵³ The extent of the scale compression is less than 1%, and absolute photoelectron energies can be obtained to an accuracy of $\pm 0.003\ \text{meV}$. The transition energy is located within a given peak by calculating the rotational contour using rotational constants for the ion and the neutral derived from molecular orbital calculations.

Materials. All reagents were purchased from commercial suppliers and were used as received. Fluorine, 5% in He, was purchased from Spectra, while deuterated and nondeuterated *m*- and *p*-bis(trimethylsilyl)benzene were prepared by quenching the corresponding Grignard reagents with chlorotrimethylsilane. 1,4-Dibromobenzene-*d*₄ was obtained from Aldrich, while deuterated 1,3-dibromobenzene was prepared by ethylaluminum dichloride catalyzed H/D exchange in the presence of C_6D_6 .⁵⁴ Other gas purities were He, 99.995% and O_2 , 99%.

Results

The 351 nm photoelectron spectra of the *o*-, *m*-, and *p*-benzyne ions, **1**⁻, **2**⁻, and **3**⁻, respectively, are shown in Figure 1, and the spectra for the deuterated ions, **1d**⁻, **2d**⁻, and **3d**⁻, are shown in Figure 2. In the following sections, we describe the features in the photoelectron spectra of the benzyne ions and the corresponding deuterated isotopomers. For each species, we provide band positions and measured vibrational frequencies, along with Franck–Condon factors for the spectral transitions.

***o*-Benzyne.** The 351 nm photoelectron spectra of **1**⁻ and **1d**⁻, shown at the tops of Figures 1 and 2, respectively, are essentially the same as the 488 nm spectra described in detail previously.⁴⁸ As in the previous study, the negative ions were prepared by the reaction of benzene and benzene-*d*₆ with the atomic oxygen ion, O^- . Two distinct features are observed in the spectra of these ions, corresponding to formation of the singlet (lower energy) and triplet (higher energy) states of *o*-benzyne. Expanded views of the singlet features are shown in the insets in Figures 1 and 2. The electron affinity for singlet **1** is found to be $0.566 \pm 0.008\ \text{eV}$, while the origin of the triplet state feature is at a binding energy of $2.194 \pm 0.008\ \text{eV}$, $1.628 \pm 0.006\ \text{eV}$ ($37.5 \pm 0.3\ \text{kcal/mol}$) above the ground state. For **1d**, we find an EA of $0.560 \pm 0.008\ \text{eV}$ and the triplet origin at $2.193 \pm 0.008\ \text{eV}$, $1.633 \pm 0.013\ \text{eV}$ ($37.7 \pm 0.3\ \text{kcal/mol}$)

(49) Bruins, A. P.; Ferrer-Correia, A. J.; Harrison, A. G.; Jennings, K. R.; Mitchum, R. K. *Adv. Mass. Spectrom.* **1978**, *7*, 355.

(50) Wenthold, P. G.; Hu, J.; Squires, R. R. *J. Am. Chem. Soc.* **1994**, *116*, 6961.

(51) Wenthold, P. G.; Hu, J.; Squires, R. R. *J. Mass Spectrom.* **1998**, in press.

(52) Neumark, D. M.; Lykke, K. R.; Andersen, T.; Lineberger, W. C. *Phys. Rev. A* **1985**, *32*, 1890.

(53) Moore, C. E. *Atomic Energy Levels*; US GPO Circular No. 467: Washington, 1952.

(54) Long, M. A.; Garnett, J. L.; Vining, R. F. W. *J. Chem. Soc., Perkin Trans. 2* **1975**, 1298.

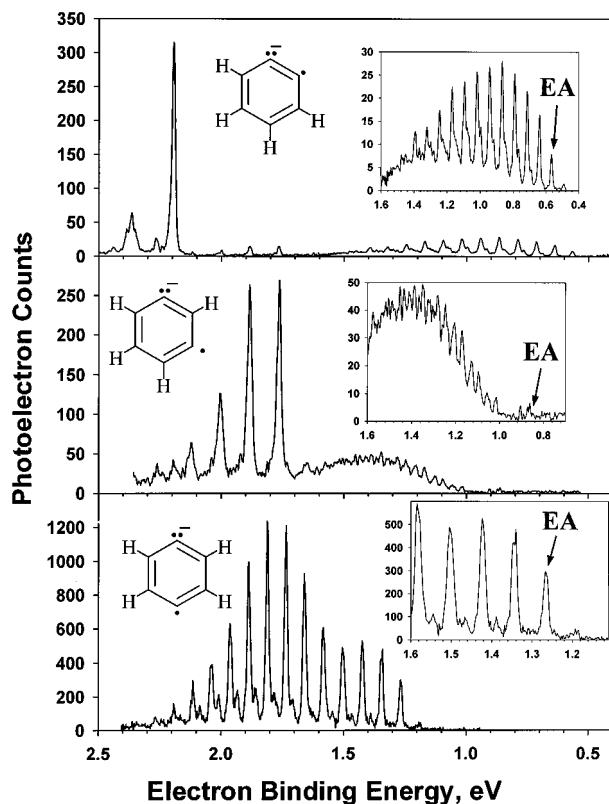


Figure 1. 351 nm photoelectron spectra of the *o*-, *m*-, and *p*-benzyne negative ions (1^- , 2^- , and 3^- , respectively) at room temperature. Electron affinities of the benzyne ions are indicated on the expanded views of the singlet regions, shown in the inserts.

above the ground state. These values differ slightly from those reported previously by LSL⁴⁸ but are well within the combined error limits of the two measurements.

Vibrational structure is observed in the spectral features for both electronic states of *o*-benzyne. As discussed by LSL,⁴⁸ the singlet feature of **1** consists of at least three vibrational progressions, corresponding to vibrational frequencies of 600, 1010, and 1860 cm^{-1} . Moreover, it was argued that accurate modeling of the singlet feature required the inclusion of a fourth vibrational mode with a frequency of 605 cm^{-1} .⁴⁸ We have modeled the singlet feature in the 351 nm photoelectron spectrum of 1^- using a Franck–Condon factor fitting routine that has been described previously.⁴⁷ The important parameters used in the fit include the position of the electronic band origin, the vibrational frequencies for the ion and the neutral, and the corresponding “normal coordinate displacements”, ΔQ_i , which correspond to the Franck–Condon factors for the transition. The frequencies and Franck–Condon factors obtained for the singlet state are listed in Table 1, and the fit to the data is shown in Figure 3. Unlike LSL,⁴⁸ we found that the fit did not improve significantly when a fourth vibrational mode was added to the model. The three vibrational frequencies obtained in this work are in good agreement with those reported previously.⁴⁸ For the singlet state feature of **1d**, two vibrational progressions are found, corresponding to frequencies of 580 and 1860 cm^{-1} . The results are summarized in Table 1.

Four vibrational frequencies are derived from the triplet state feature of **1**: 560 \pm 20, 1275 \pm 30, 1395 \pm 30, and 1520 \pm 40 cm^{-1} . The 560 and 1395 cm^{-1} frequencies obtained in this work correspond to the 570 and 1440 cm^{-1} frequencies derived by LSL from the 488 nm photoelectron spectrum.⁴⁸ The Franck–Condon factors calculated for the four modes identified

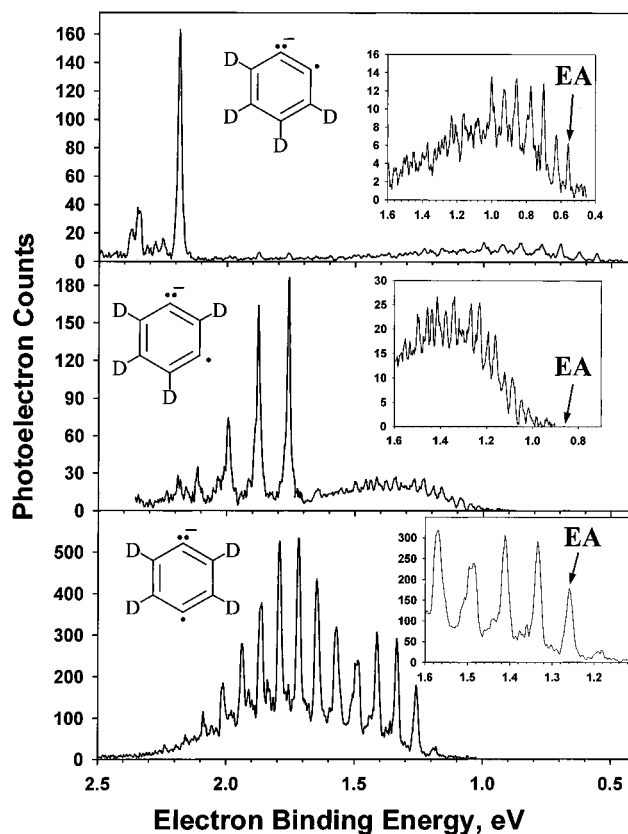


Figure 2. 351 nm photoelectron spectra of the deuterated benzyne ions ($1d^-$, $2d^-$, and $3d^-$) at room temperature. Electron affinities of the benzyne ions are indicated on the expanded views of the singlet regions, shown in the inserts.

above are 0.101, 0.088, 0.085, and 0.070 $\text{\AA} \text{amu}^{1/2}$, respectively. These indicate only a small geometry difference between the ion 1^- and triplet *o*-benzyne. The calculated spectrum obtained for the triplet state of **1** is shown in Figure 3. For the triplet state of **1d**, only two vibrational progressions are observed, corresponding to frequencies of 1265 \pm 30 and 1515 \pm 30 cm^{-1} . The Franck–Condon factors calculated for these modes are 0.126 and 0.088 $\text{\AA} \text{amu}^{1/2}$, respectively. A summary of all the observed vibrations and corresponding Franck–Condon factors is provided in Table 1.

Hot bands are observed in both the singlet and triplet state features of **1**, which correspond to transitions from $\nu = 1$ in 1^- . A frequency of 610 \pm 20 cm^{-1} is derived from the singlet feature, while a value of 595 \pm 30 cm^{-1} is obtained from the triplet feature. These likely refer to the same mode in the ion, which has a frequency of about 600 cm^{-1} .

In addition to the singlet and triplet features in the photoelectron spectra of 1^- and $1d^-$, we also observe weak features in the region of 1.7–2.3 eV. These features have been observed previously⁴⁸ and were attributed to contamination by either the *m*- or *p*-benzyne ion isomers. In the following section, we show that the signal comes from *m*-benzyne ion, 2^- .

***m*-Benzyne.** The 351 nm photoelectron spectrum of the *m*-benzyne negative ion, 2^- , prepared according to eq 2a is shown in the middle panel of Figure 1. The spectrum obtained for the deuterated isomer, $2d^-$ (Figure 2) is essentially the same as that for 2^- . Photodetachment to two electronic states is evident in these spectra, with two distinct features beginning at ca. 1.0 and 1.7 eV. Considering that high-level ab initio calculations predict a singlet–triplet splitting for **2** around 0.7–0.9 eV,^{40,46} we assign the two bands to the singlet and triplet states of *m*-benzyne, respectively.

Table 1. Band Origin Positions and Measured Vibrational Modes Obtained from Photoelectron Spectra of *o*-, *m*-, and *p*-Benzyne Negative Ions

	<i>o</i> -benzyne		<i>m</i> -benzyne		<i>p</i> -benzyne	
	C ₆ H ₄	C ₆ D ₄	C ₆ H ₄	C ₆ D ₄	C ₆ H ₄	C ₆ D ₄
<i>singlet</i> origin, eV (electron affinity)	0.566 ± 0.008 0.560 ± 0.010 ^c 0.564 ± 0.007 ^d	0.560 ± 0.008 0.551 ± 0.010 ^c 0.556 ± 0.008 ^d	0.852 ± 0.011 ^{a,b}	<i>a</i>	1.265 ± 0.008	1.260 ± 0.008
<i>triplet</i> origin, eV Δ <i>E</i> _{<i>singlet</i>–<i>triplet</i>} , eV (kcal/mol)	2.194 ± 0.008 1.628 ± 0.013 (37.5 ± 0.3) (37.7 ± 0.6) ^c (37.5 ± 0.3) ^d	2.193 ± 0.008 1.633 ± 0.013 (37.6 ± 0.3) (37.9 ± 0.3) ^c (37.7 ± 0.3) ^d	1.763 ± 0.008 0.911 ± 0.014 (21.0 ± 0.3)	1.760 ± 0.008	1.430 ± 0.015 ^e 0.165 ± 0.016 (3.8 ± 0.4)	1.427 ± 0.015 ^e 0.167 ± 0.016 (3.9 ± 0.4)
<i>singlet</i> vibrations, cm ⁻¹ (Δ <i>Q</i> _i , Å amu ^{1/2})	600 ± 15 (0.51) 1010 ± 40 (0.18) 1860 (0.24)	580 ± 20 (0.52) 1860 (0.21)	~300 ^f	~300 ^f	635 ± 20 (0.44) 990 ± 20 (0.14)	615 ± 20 (0.43)
<i>triplet</i> vibrations, cm ⁻¹ (Δ <i>Q</i> _i , Å amu ^{1/2})	560 ± 20 (0.10) 1275 ± 30 (0.09) 1395 ± 30 (0.09) 1520 ± 40 (0.09)	1265 ± 30 (0.13) 1515 ± 40 (0.09)	970 ± 15 (0.28)	955 ± 20 (0.26)	610 ± 15 (0.76) 995 ± 20 (0.12)	590 ± 20 (0.75) 945 ± 40 (0.16)
<i>ion</i> vibration, cm ⁻¹	600 ± 30		885 ± 20	910 ± 40	615 ± 30	605 ± 30

^a Not accessed in photoelectron spectrum. ^b Electron affinity taken from collision-induced dissociation branching ratios; see ref 28. ^c Reference 48. ^d Weighted average of two measurements; recommended value. ^e Triplet origin obtained from modeling procedures described in text. ^f Does not contain a regular vibrational progression.

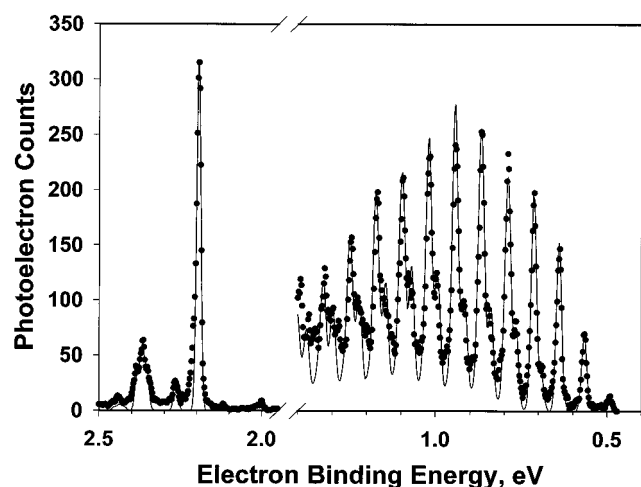


Figure 3. Franck–Condon fits of the singlet and triplet regions in the spectrum of **1**⁻. The experimental data are shown as filled circles, and the line is calculated using the parameters listed in Table 1.

The lower energy, singlet bands in the spectra for **2**⁻ and **2d**⁻ appear to consist of extended vibrational progressions with a frequency around 300 cm⁻¹ (see insets). The lowest energy peak observable in the spectrum of **2**⁻ occurs at an electron binding energy of ca. 0.99 eV, but it is unlikely that this corresponds to the origin. The nature of the vibrational progression suggests that the origin for this feature is much lower in energy and of too low intensity to be observed. This indicates that the Franck–Condon factors for transition between the ion and neutral states are small due to a large difference in their geometries. From the observed spectra, we can only assign *upper limits* to the electron affinities for **2** and **2d** of 0.99 and 1.02 eV. The higher upper limit assigned for **2d** is a result of poorer signal-to-noise in photoelectron spectrum of **2d**⁻.

The higher binding energy features in the spectra of **2**⁻ and **2d**⁻ are assigned to formation of the triplet states. The origin of the triplet band is found at an electron binding energy of 1.763 ± 0.008 eV in the spectrum of **2**⁻ and at 1.760 ± 0.008 eV in the spectrum of **2d**⁻. Vibrational activity is also evident in the triplet state feature for *m*-benzyne, but the extent of the activity is less than that observed for the singlet state. This indicates that the geometry of the triplet state is much closer to that of the anion than is the geometry of the singlet. A single

vibrational mode with a frequency of 970 ± 15 cm⁻¹ is derived from the triplet band for **2**, while a frequency of 955 ± 20 cm⁻¹ is derived for triplet **2d**. The peak positions and intensities for the triplet feature can be accurately modeled using a single active vibrational mode and Franck–Condon factors of 0.28 and 0.26 Å amu^{1/2} for **2** and **2d**, respectively. The relative intensities of the peaks calculated for the triplet state of **2** using a vibrational frequency of 970 cm⁻¹ and Δ*Q*_i = 0.28 Å amu^{1/2} are 1.00/0.99/0.54/0.21, which agree well with the measured relative intensities of 1.00/0.98/0.49/0.24. Hot bands observed in the triplet region indicate vibrational frequencies of 885 ± 20 and 910 ± 40 cm⁻¹ for **2**⁻ and **2d**⁻, respectively. The fitting parameters are summarized in Table 1.

In their earlier report of the 488 nm photoelectron spectra of **1**⁻ and **1d**⁻, LSL⁴⁸ noted the presence of weak spectral features with origin peaks at electron binding energies of 1.761 and 1.759 eV, respectively. Vibrational progressions were also observed, corresponding to frequencies of 980 and 960 cm⁻¹, respectively. LSL tentatively assigned these features to *m*- or *p*-benzyne ion impurities formed by O⁻ reaction. We also observe these features in the 351 nm photoelectron spectrum of **1**⁻, as described above. The positions of these features coincide with what is observed for the triplet states of **2** and **2d**, which confirms the origins of these bands as *m*-benzyne ion impurities in the *o*-benzyne ion beam.

***p*-Benzyne.** The spectra for the *p*-benzyne negative ions, **3**⁻ and **3d**⁻, are shown at the bottom of Figures 1 and 2, respectively. Unlike the spectra for **1**⁻ and **2**⁻, the photoelectron spectrum for the *p*-benzyne ion is extremely congested. Two different electronic bands are discernible in the spectrum, but they are extensively overlapped, making interpretation difficult. That the origin region is congested is not surprising in view of the small singlet–triplet splitting predicted for *p*-benzyne.⁴⁰

Photodetachment of **3**⁻ to two distinct electronic states of **3** can be verified by photoelectron angular distribution measurements. The spectrum shown in Figure 1 was obtained with use of the “magic angle”, where the laser electric field vector is polarized by 54.7° with respect to the electron detector. Spectra for **3**⁻ were also measured with laser polarizations of θ = 0° and θ = 90°. These spectra are shown in Figure 4 as solid and dotted lines, respectively. A clear difference is observed between the two states for the two laser polarizations, with the

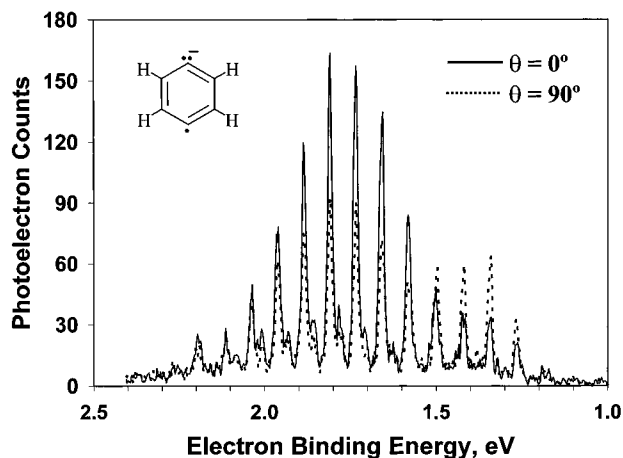


Figure 4. Photoelectron spectra of 3^- obtained with the laser polarization at 0° (solid line) and 90° (dashed line), measured under similar experimental conditions.

lower energy peaks being more prominent when $\theta = 90^\circ$. In principle, it is possible to scale and subtract the two different spectra shown in Figure 4 in order to deconvolute the shapes of the two different electronic features. For example, Gilles et al. used this approach in their analyses of the photoelectron spectra of halocarbenes ions, HCX^- .⁵⁵ Unfortunately, the deconvoluted spectrum obtained by scaling and subtracting the spectra shown in Figure 4 is so noisy that it does not provide additional information that cannot be obtained from the spectra measured at the magic angle. Therefore, the spectra for 3^- and $3d^-$ shown in Figures 1 and 2 were used for all further analyses. The origin of the lower energy band (shown in the inset in Figure 1) is assigned to be the peak occurring at an electron binding energy of 1.265 ± 0.008 eV. This corresponds to the adiabatic electron affinity of singlet 3 . Two different vibrational progressions are observed in the singlet feature, with frequencies of 635 ± 20 and 990 ± 20 cm^{-1} . A hot band is also observed 615 ± 30 cm^{-1} from the origin, which corresponds to an excited vibrational mode of 3^- . From the spectrum of the deuterated ion $3d^-$ (Figure 2), we find $\text{EA}(3d) = 1.260 \pm 0.008$ eV and vibrational frequencies of 605 ± 30 cm^{-1} for the ion and 615 ± 20 cm^{-1} for the neutral.

The higher energy feature in the spectrum of the *p*-benzyne ion is assigned to the triplet state of 3 . This feature consists of an extended vibrational progression with its origin buried within the singlet manifold. Several different analytical methods were employed to identify the peak corresponding to the origin of the triplet state. First, the positions of the peaks in the spectra of the deuterated and undeuterated ions were compared. The difference in the vibrational spacing in the two spectra will lead to slightly different positions for the vibrational peaks, but the origin peaks of the two bands will be at essentially the same energy, separated only by the difference in zero point energies for the deuterated and undeuterated systems. This difference is expected to be small, on the order of 3 meV or less, as is found for the singlet band. Unfortunately, the peaks near the triplet origin in the spectrum have such low intensities and are so poorly resolved from the peaks of the singlet band that their positions cannot be measured directly with the required accuracy. However, it is possible to use the vibrational spacings for the more intense, higher energy peaks in the progression to estimate the positions of the lower energy peaks. Using the positions of the peaks in the main progression from ca. 1.6–

Table 2. Observed and Extrapolated^a Peak Positions for the Triplet Region of 3 and $3d$

<i>p</i> -benzyne (3) ^b	<i>p</i> -benzyne- <i>d</i> ₄ ($3d$) ^b	<i>p</i> -benzyne (3) ^b	<i>p</i> -benzyne- <i>d</i> ₄ ($3d$) ^b
2.038	2.012	(1.582)	(1.573)
1.961	1.938	(1.506)	(1.500)
1.886	1.866	(1.430)	(1.427)
1.810	1.792	(1.354)	(1.354)
1.734	1.718	(1.279)	(1.281)
1.658	1.646		

^a In parentheses. ^b Electron binding energies in eV.

2.3 eV in the spectrum of 3^- (Table 2), we obtain an average peak spacing of 76 meV (612 cm^{-1}). This value can then be used to predict the positions of the lower energy peaks in the triplet feature. These are listed in parentheses in Table 2.

A similar exercise was carried out with the spectrum for $3d^-$ (Figure 2). The peak positions for the higher energy portion of the main progression in the triplet region (Table 2) give an average peak spacing of 73 meV (590 cm^{-1}). This value was used to calculate the lower energy peak positions shown in parentheses in Table 2.

To find the triplet origin, we compare the positions of the lowest energy triplet peaks in the spectra of 3^- and $3d^-$. The two vibrational series listed in Table 2 converge near the peak at ~ 1.35 eV. We consider this the most likely region to find the origin, with the peaks at 1.43, 1.35, or 1.28 eV being the most likely candidates. It is important to note that all three candidate peaks are higher in energy than the origin of the lower energy band. This provides support for the assignment of the higher energy band to the triplet state of *p*-benzyne, because the singlet state of *p*-benzyne is generally believed to be slightly lower in energy than the triplet state.^{39,40} Accepting these state assignments, we can use additional modeling to determine the triplet origin more precisely. The Franck–Condon factors for an electronic transition can be calculated if the geometries and the force constants for the normal modes of the initial and final states are known. Experimentally determined geometries and force constants are not available for reactive intermediates such as the benzyne and benzyne anions. However, it has been shown that estimates of these properties obtained from ab initio calculations can be of sufficient accuracy for modeling photoelectron spectra.⁵⁶ For example, Chen and co-workers used the results of ab initio calculations to locate the origin in the photoelectron spectrum of CCl_2 ,⁵⁷ and Wenthold et al. demonstrated that the photoelectron spectrum of allyl anion could be accurately modeled with use of geometries and frequencies determined at the MP2/6-31+G* level of theory.⁵⁸ In the present work, we have used the ab initio results for D_{2h} 3^- and D_{2h} 3 reported previously^{39,46} to estimate the Franck–Condon factors for photodetachment. A detailed account of the procedure is provided elsewhere;⁵⁸ it involves a calculation of the Duschinsky \mathbf{K} matrix for the transition, from which the Franck–Condon factors can be derived. The \mathbf{K} matrix is calculated with use of a software package developed by Chen and co-workers that uses the output file from a frequency calculation performed with the Gaussian 94 suite of programs.⁵⁹

The triplet state bands in the *o*- and *m*-benzyne ion spectra were calculated first in order to calibrate the performance of this modeling procedure for these types of systems. In the *o*-

(56) Chen, P. In *Unimolecular and Bimolecular Reaction Dynamics*; Ng, C. Y., Baer, T., Powis, I., Eds.; John Wiley & Sons: New York, 1994.

(57) Kohn, D. W.; Robles, E. S. J.; Logan, C. F.; Chen, P. *J. Phys. Chem.* **1993**, *97*, 4936.

(58) Wenthold, P. G.; Polak, M. L.; Lineberger, W. C. *J. Phys. Chem.* **1996**, *100*, 6920.

(55) Gilles, M. K.; Ervin, K. M.; Ho, J.; Lineberger, W. C. *J. Phys. Chem.* **1992**, *96*, 1130.

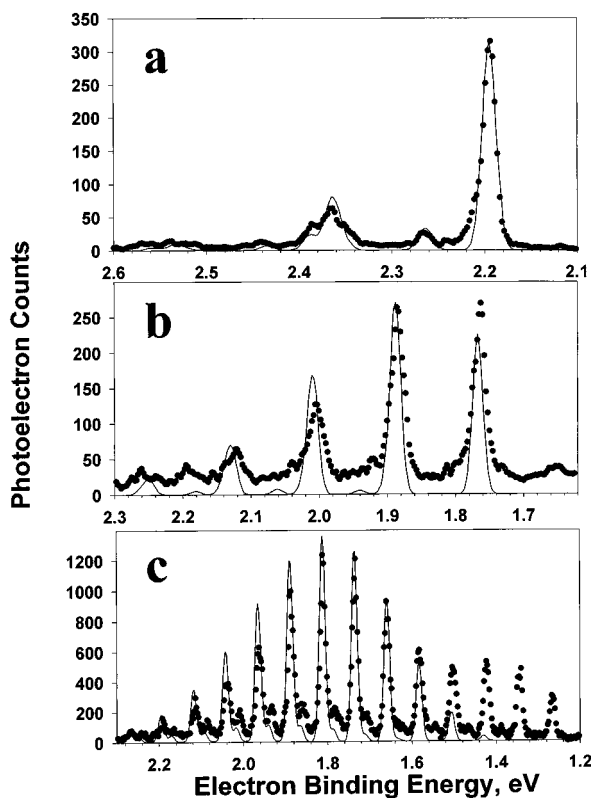


Figure 5. Features for the triplet regions of the photoelectron spectra of 1^- , 2^- , and 3^- , obtained using geometries and vibrational modes for the ions and the triplet states calculated at the B3LYP/cc-pVDZ level of theory. The energies of the origin peaks were set to match the measured origin positions. The calculated spectrum is shown as a solid line, and the measured data are shown as filled circles.

and *m*-benzyne ion spectra, the triplet features are well-separated from the singlet features, and independent assignments of the triplet state origins are available. The spectra calculated with use of the geometries and force constants for the ions and triplet biradicals obtained from B3LYP/cc-pVDZ calculations are shown as solid lines in Figure 5a and 5b. Excellent agreement is achieved between the experimental data (shown as darkened circles) and the calculated spectra, i.e., all the prominent spectral features and peak-positions are correctly reproduced by the model. This indicates that the geometries and force constants for benzyne triplets and benzyne negative ions provided by B3LYP/cc-pVDZ calculations are sufficiently accurate for reliable modeling of the photoelectron spectra.

Having established the validity of the modeling procedure, we then calculated the triplet portion of the *p*-benzyne ion spectrum using the B3LYP/cc-pVDZ geometries and force constants for 3 and 3^- . The result is shown as the solid line in Figure 5c. The computed spectrum reproduces the positions of the higher energy features of the experimental spectrum (shown as darkened circles) extremely well. Minor discrepancies are evident in the highest energy portion of the spectra, where the peak intensities are slightly overestimated by the model. This is likely due to the harmonic oscillator approxima-

tion used for deriving the peak intensities from the Franck–Condon factors, since anharmonic contributions can become significant at energies far above the origin.

The only adjustable parameters used for the modeling procedure described above were the height and position of the origin peak. The triplet origin used for the calculated spectrum shown in Figure 5c corresponds to an electron binding energy of 1.430 eV, which coincides with the region where the vibrational progressions in the *p*-benzyne and *p*-benzyne-*d*₄ spectra converge (Table 2). Shifting the origin lower by one quantum of energy in the 612 cm⁻¹ vibrational mode leads to a better fit of the high energy portion of the spectrum but results in a significant overestimation of the intensities of the lower energy peaks, which we should be able to model more accurately. Attempts using other values for the energy of the triplet origin give substantially poorer fits to the data. Therefore, we conclude that the origin is most likely at 1.430 eV, but we cannot completely rule out the possibility of the origin lying one quantum of vibrational energy lower (1.354 eV). An uncertainty of 0.015 eV is assigned to the energy of the triplet origin to account for the possible accumulation of errors that may arise from extrapolating the vibrational series to lower energy.

From the energy difference between the assigned origins for the singlet band (1.265 ± 0.008 eV) and the triplet band (1.430 ± 0.015 eV), we obtain a singlet–triplet splitting for *p*-benzyne, $\Delta E_{ST}(3)$, of 0.165 ± 0.016 eV (3.8 ± 0.4 kcal/mol). With the unlikely possibility that the triplet origin lies one vibrational quantum (0.076 eV) lower in energy than the preferred value, one obtains a value for $\Delta E_{ST}(3)$ of 0.089 ± 0.016 eV (2.1 ± 0.4 kcal/mol).

The peak corresponding to the triplet origin in the spectrum of $3d^-$ occurs at 1.427 eV, 3 meV lower than the triplet origin for 3 (Table 2). This isotope shift is similar to what is found for the singlet state of 3 , where the electron binding energies of the deuterated and undeuterated ions differ by 5 meV. As with 3 , we assign an uncertainty of 0.015 eV to the triplet origin for $3d^-$. From the energy difference between the singlet and triplet origin peaks in the photoelectron spectrum $3d^-$ we obtain a value for $\Delta E_{ST}(3d)$ of 0.167 ± 0.016 eV (3.9 ± 0.4 kcal/mol). A singlet–triplet splitting that is lower by one quantum of energy in the 590 cm⁻¹ vibrational mode (0.073 eV) cannot be ruled out but is considered unlikely.

Vibrational frequencies for the triplet states of *p*-benzyne and *p*-benzyne-*d*₄ can be obtained from the photoelectron spectra. From the peak spacings in the spectrum of 3^- , we assign vibrational frequencies of 610 ± 15 and 995 ± 20 cm⁻¹. Corresponding modes with frequencies of 590 ± 20 and 945 ± 40 cm⁻¹ are obtained for the triplet state of $3d$.

Finally, the peak positions and intensities in the photoelectron spectrum of 3^- can also be modeled using the Franck–Condon factor fitting procedure employed by LSL in their analysis of the photoelectron spectrum of *o*-benzyne ion. The singlet region in the spectrum of 3^- was modeled by using only the origin peak and the $\nu = 1$ peak in order to avoid possible contributions from the triplet state. The isolated triplet band was obtained by subtracting the calculated singlet spectrum from the experimental photoelectron spectrum. The deconvoluted triplet band was then fit in the same manner as the singlet band. The Franck–Condon factors obtained from the fits of the singlet and triplet bands are listed in Table 1. The overall spectrum, obtained by summing the calculated singlet and triplet spectra, displays a good match with the experimental data, as shown in Figure 6. We emphasize the difference between this fitting

(59) Gaussian 94; Frisch, M. J.; Trucks, G. W.; Schlegel, H. B.; Gill, P. M. W.; Johnson, B. G.; Robb, M. A.; Cheeseman, J. R.; Keith, T.; Petersson, G. A.; Montgomery, J. A.; Raghavachari, K.; Al-Laham, M. A.; Zakrewski, V. G.; Ortiz, J. V.; Foresman, J. B.; Cioslowski, J.; Stefanov, B. B.; Nanayakkara, A.; Challacombe, M.; Peng, C. Y.; Ayala, P. Y.; Chen, W.; Wong, M. W.; Andres, J. L.; Replogle, E. S.; Gomperts, R.; Martin, R. L.; Fox, D. J.; Binkley, J. S.; Defrees, D. J.; Baker, J. J.; Baker, J. J.; Stewart, J. J. P.; Head-Gordon, M.; Gonzalez, C.; Pople, J. A., Gaussian, Inc.: Pittsburgh, PA, 1994.

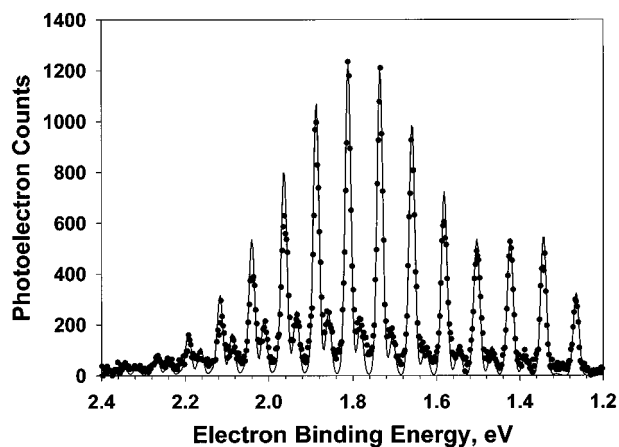


Figure 6. Franck-Condon fit of the photoelectron spectrum of 3^- . The experimental data are shown as filled circles, and the line is calculated by summing the fits of the singlet and triplet regions using the parameters listed in Table 1. A value for the singlet-triplet splitting of *p*-benzyne of 3.8 kcal/mol was used to generate the fit shown in the figure.

procedure, in which an analytical fit of the data yields empirical values of the Franck-Condon factors, and the fitting procedure described above, in which the Franck-Condon factors used to calculate the spectra are derived from geometries and force constants estimated from *ab initio* calculations.

Discussion

This study provides new thermochemical and spectroscopic data for the benzyne, including the first experimental measurements of the singlet-triplet splittings of the *meta* and *para* isomers. In this section, we summarize the procedures used to identify and distinguish the isomeric benzyne ions and then discuss the important features of the photoelectron spectra, along with some implications of the physical quantities that can be derived from these spectra.

Ion Structures. The negative ions required for this study were prepared using synthetic procedures that have been described previously,^{24,26,28,49,50,60} and details of the identification of the ions have been provided.^{24,28} Preparation of *o*-benzyne ion, 1^- , by the reaction of benzene with O^- (eq 1) was first reported Bruins et al.⁴⁹ nearly 20 years ago. Gas-phase synthesis of *m*- and *p*-benzyne ions, 2^- and 3^- respectively, by the reaction of *m*- and *p*-trimethylsilylphenyl anions with F_2 (eq 2) was achieved only recently.^{28,50} The isomeric structures of ions 1^- , 2^- , and 3^- prepared by these methods were authenticated by a gas-phase chemical derivatization procedure used in combination with tandem mass spectrometry.²⁸ Sequential ion/molecule reactions of each benzyne ion, first with CO_2 and then with NO_2 , yields the corresponding *o*-, *m*-, or *p*-nitrobenzoate ion derivative, $O_2NC_6H_4CO_2^-$. Each derivative ion displayed an apparent basicity that was identical to that of the authentic *o*-, *m*-, or *p*-nitrobenzoate ion prepared from the corresponding neutral nitrobenzoic acid. The photoelectron spectra obtained in the present study further support the conclusion that the benzyne negative ions formed by the reactions shown in eq 1 and 2 are distinct, noninterconverting isomers.²⁸ The photoelectron spectrum for each isomer is completely distinct and does not contain any significant features attributable to other isomers, with the exception of the aforementioned *m*-benzyne ion contamination in the spectrum of 1^- . An important observation is that the spectra for 2^- and 3^- , the higher energy benzyne ion isomers,²⁸ do not display any contamination from

1^- , the lowest energy benzyne ion. Therefore, isomerization of 2^- and 3^- , by either unimolecular or bimolecular reactions, is unimportant under the conditions of our experiments.

In the earlier report of the chemistry of the *m*- and *p*-benzyne ions,^{28,50} it was noted that formation of these ions by the desilylation method in a flowing afterglow apparatus (eq 2) also produces phenyl anion ($C_6H_5^-$, *m/z* 77) and dihydrophenyl anion ($C_6H_3^-$, *m/z* 75) as significant side products. Because the mass resolution of the Wien filter in the photoelectron spectrometer is not sufficient to resolve the peaks in this region ($M/\Delta M \approx 30$), it is possible that photoelectron signals from the $C_6H_5^-$ and $C_6H_3^-$ ions could contaminate the $C_6H_4^-$ photoelectron spectra. The measured photoelectron spectrum for 3^- does contain a small contribution from phenyl anion, as indicated by the presence of a peak at 1.096 eV, which is the origin peak in the spectrum of phenyl anion.⁶¹ For this reason, a scaled spectrum obtained for authentic phenyl anion was subtracted from the measured spectrum for 3^- to give resulting spectrum shown at the bottom of Figure 3. However, the total photoelectron signal due to phenyl anion is less than 0.1% of the total signal, which indicates that $C_6H_5^-$ is not formed to an appreciable extent under the conditions of our experiments. No photoelectron signal attributable to an ion with *m/z* 75 is observed.

Electron Affinities and Singlet-Triplet Splittings. The adiabatic electron affinities of *o*- and *p*-benzyne can be obtained directly from the photoelectron spectra, because the singlet features for these species have well-defined origin peaks. The electron affinities of *o*-benzyne and *o*-benzyne-*d*₄ obtained in the present study are 0.566 ± 0.008 eV and 0.560 ± 0.008 eV, respectively, which are slightly higher than the values reported by LSL, 0.560 ± 0.010 eV and 0.551 ± 0.010 eV,⁴⁸ but still within the quoted error limits. For the final values of the electron affinities of 1 and $1d$, we use the weighted average of the two measurements, 0.564 ± 0.007 and 0.556 ± 0.008 eV, respectively, where the smaller uncertainties are derived by standard statistical treatments.⁶² The singlet-triplet splittings of 1 and $1d$ are determined by the present measurements to be 37.5 ± 0.3 and 37.6 ± 0.3 kcal/mol, respectively. LSL⁴⁸ assigned values of 37.7 ± 0.6 and 37.9 ± 0.6 kcal/mol, respectively, in good agreement with the present results. Again, we use the weighted averages from the two measurements and recommend final values for the singlet-triplet splittings of 1 and $1d$ of 37.5 ± 0.3 and 37.7 ± 0.3 kcal/mol, respectively.

The electron affinities of *p*-benzyne and *p*-benzyne-*d*₄ are determined to be 1.265 ± 0.008 and 1.260 ± 0.008 eV, respectively, from the position of the origin peak in each singlet feature. The measured EA of *p*-benzyne is somewhat higher than that of phenyl radical, 1.096 eV, which was also determined by photoelectron spectroscopy.⁶¹ This indicates a small stabilizing effect due to odd-spin and negative charge delocalization between the two dehydro centers in *p*-benzyne ion, as was predicted earlier by *ab initio* calculations.³⁹ The value for EA- (3) determined by photoelectron spectroscopy is in excellent agreement with the value of 1.249 ± 0.022 eV obtained by Wenthold, Hu, and Squires from the kinetic method.²⁸ In these experiments, electron affinities are estimated from a quantitative relationship between electron binding energies of hydrocarbon ions (R^-) and the measured fragment ion yield ratios obtained

(60) Lee, J.; Grabowski, J. J. *Chem. Rev.* **1992**, 92, 1611.

(61) Gunion, R. F.; Gilles, M. K.; Polak, M. L.; Lineberger, W. C. *Int. J. Mass Spectrom. Ion Processes* **1992**, 117, 601.

(62) Bevington, P. R. *Data Reduction and Error Analysis for the Physical Sciences*; McGraw-Hill: New York, 1969.

from collision-induced dissociation (CID) of the corresponding sulfur dioxide adducts (RSO_2^-). The relationship is calibrated with the results for hydrocarbon ions having well-established electron binding energies. For the experiments involving benzyne ions, the relative yields of C_6H_4^- and SO_2^- obtained from CID of the three different $\text{C}_6\text{H}_4\text{SO}_2^-$ adducts were measured, along with the $\text{C}_6\text{H}_5^-/\text{SO}_2^-$ yield ratio resulting from CID of the SO_2 adduct of phenyl anion. The CID ratios obtained for the *o*-benzyne ion and phenyl anion adducts were used to calibrate the EA relationship, and the electron affinities for *m*- and *p*-benzyne were derived. The excellent agreement between the two independent EA determinations for *p*-benzyne suggests that the kinetic method provides a reliable means for determining electron affinities of the benzyne.

The singlet–triplet splitting of *p*-benzyne is determined from the difference in energy between the singlet and triplet origin peaks. The singlet origin was taken directly from the spectrum, while the triplet origin was located with the aid of the modeling procedures described in the results section. We assign a value of 3.8 ± 0.4 kcal/mol for $\Delta E_{\text{ST}}(\mathbf{3})$. An alternative value of 2.1 ± 0.4 kcal/mol, which differs from the preferred value by one quantum of vibrational energy in the active mode, cannot be ruled out but is considered unlikely. Similarly, the singlet–triplet splitting of deuterated *p*-benzyne $\mathbf{3d}$ is assigned to be 3.9 ± 0.4 kcal/mol, although an alternative value of 2.2 ± 0.4 kcal/mol is possible.

The adiabatic electron affinity of *m*-benzyne cannot be obtained directly from the photoelectron spectrum of $\mathbf{2}^-$ because the singlet origin is not observed. Moreover, because of the uncertainties in the geometry and vibrational frequencies obtained for $\mathbf{2}$ from ab initio calculations (vide infra), it is not possible to identify the origin using a modeling procedure similar to that used for the triplet state of $\mathbf{3}$. Instead, all that can be obtained is an upper limit to EA($\mathbf{2}$) of 0.99 eV. Similarly, the spectrum of $\mathbf{2d}^-$ indicates EA($\mathbf{2d}$) < 1.01 eV. Therefore, we must rely on the electron affinity of *m*-benzyne obtained from the kinetic method experiments, as described above. However, with an accurate EA for *p*-benzyne now available from the present work, we can further refine the quantitative relationship between electron affinities and CID fragment ratios. The modified calibration equation obtained using the EAs of phenyl radical (1.096 ± 0.006 eV),⁶¹ *o*-benzyne (0.564 ± 0.007 eV), and *p*-benzyne (1.265 ± 0.008 eV) and the reported CID fragment ratios ($r = 3.74 \pm 0.39$, 0.032 ± 0.003 , and 14.8 ± 1.7 , respectively)²⁸ is shown in eq 3. It is essentially the same as the calibration equation used earlier by Wenthold, Hu, and

$$\text{EA} = (22.0 \pm 0.2 \text{ kcal/mol}) + (2.60 \pm 0.07 \text{ kcal/mol}) \ln r \quad (1)$$

Squires, differing only in the value of the constant term by < 1%. Using eq 3 along with the published CID fragment ratio for the SO_2 adduct of $\mathbf{2}^-$, 0.408 ± 0.027 ,²⁸ we calculate EA($\mathbf{2}$) = 19.6 ± 0.3 kcal/mol (0.852 ± 0.011 eV). The singlet–triplet splitting of *m*-benzyne is given by the difference between the adiabatic EA and electron binding energy of the triplet state, 1.763 ± 0.008 eV. $\Delta E_{\text{ST}}(\mathbf{2})$ is thus determined to be 21.0 ± 0.3 kcal/mol.

We compare the measured S–T splittings for $\mathbf{1}$ – $\mathbf{3}$ with the values derived from recent ab initio calculations. Reliable predictions of the singlet–triplet splittings of the benzyne by a single computational procedure have been difficult to achieve because of the variable biradical character of these molecules. Dynamic electron correlation effects have been shown to be

significant, and the predicted splittings can be quite sensitive to the size of the basis set used for the calculations. The theoretically predicted values for the singlet–triplet splittings of the benzyne obtained at the MCSCF,⁴⁶ CASPT2,⁴⁰ CCSD(T),⁴⁰ CISD,^{46,63} and CCCI⁴⁶ levels of theory with double- ζ quality or better basis sets are in qualitative agreement with the experimental values, but systematically too low. The calculated values derived from these methods range from 32 to 37 kcal/mol for $\mathbf{1}$, 15–21 kcal/mol for $\mathbf{2}$, and 2.1–3.8 kcal/mol for $\mathbf{3}$. The highest values in each of these ranges are actually in quite good agreement with the experimental values, but each was derived from a different computational procedure. As noted recently by Cramer, Nash, and Squires,⁴⁰ CCSD(T)/cc-pVTZ calculations show the best overall performance with respect to calculated singlet–triplet splittings, giving values for $\mathbf{1}$ – $\mathbf{3}$ of 35.3, 20.7, and 2.3 kcal/mol, respectively.

Vibrational Assignments. In this section, we consider the vibrational structure observed in the photoelectron spectrum of the benzyne ions and make assignments for each of the active vibrational modes. Active vibrational modes in a negative ion photoelectron spectrum correspond to totally symmetric modes in the anion and result from geometry differences between the ion and the neutral.

***o*-Benzyne.** The active vibrational modes in the photoelectron spectrum of *o*-benzyne ion have been discussed previously.⁴⁸ For the singlet state, three modes are active. These include a ring deformation mode with $\nu = 600 \text{ cm}^{-1}$, which is similar to ν_{6a} in benzene (Wilson numbering),⁶⁴ a ring breathing mode with $\nu = 1010 \text{ cm}^{-1}$, and a C \equiv C stretching mode with $\nu = 1860 \text{ cm}^{-1}$. Only the ring deformation and ring breathing modes are immediately apparent in the singlet region because the C \equiv C stretching mode is coincident with $\nu = 3$ in the ring deformation mode. However, the spectrum cannot be adequately fit without including the C \equiv C mode in the model. The measured frequencies for singlet $\mathbf{1}$ are in excellent agreement with those obtained by IR spectroscopy of the matrix-isolated molecule.³⁵ The ring deformation frequencies, found to be 600 and 580 cm^{-1} for $\mathbf{1}$ and $\mathbf{1d}$, respectively, were determined to be 589 and 579 cm^{-1} , respectively, from the matrix-IR spectrum. The C \equiv C stretching frequency, assigned to be 1860 cm^{-1} for both $\mathbf{1}$ and $\mathbf{1d}$ from the photoelectron spectrum, agrees well with the IR values of 1844–1846 cm^{-1} . The ring breathing frequencies, 1010 cm^{-1} for $\mathbf{1}$ and 980 cm^{-1} for $\mathbf{1d}$,⁴⁸ most likely correspond to the “ring stretching frequencies” at 1039 and 995 cm^{-1} , respectively, in the matrix IR spectrum.

For triplet *o*-benzyne, LSL⁴⁸ reported two vibrational modes with frequencies of $570 \pm 30 \text{ cm}^{-1}$ and $1440 \pm 30 \text{ cm}^{-1}$. In the 351 nm photoelectron spectrum, four vibrational modes are identified, with frequencies of 560 ± 20 , 1275 ± 30 , 1395 ± 30 , and $1520 \pm 40 \text{ cm}^{-1}$. The additional modes identified in the present work are near the region in the 488 nm spectrum where the analyzer begins to cut off, which makes them difficult to observe at that wavelength. They do appear as perceptible peak-shoulders in the 488 nm spectrum.⁴⁸ The 560 and 1395 cm^{-1} frequencies identified in this study correspond to the two frequencies reported by LSL.⁴⁸ The 560 cm^{-1} frequency is readily assigned to a ring deformation mode, analogous to that described above for the singlet. The frequencies of the other modes observed for triplet $\mathbf{1}$ are also likely due to ring deformation. These frequencies were assigned with the aid of molecular orbital calculations. Optimized geometries and harmonic vibrational frequencies have been determined for $\mathbf{1}^-$

(63) Nicolaidis, A.; Borden, W. T. *J. Am. Chem. Soc.* **1993**, *115*, 11951.

(64) Wilson, E. B., Jr. *Phys. Rev.* **1934**, *45*, 706.

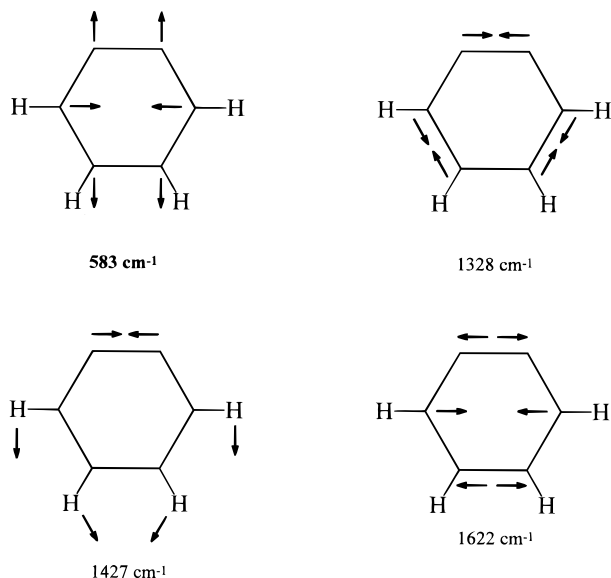


Figure 7. The active vibrational modes for triplet **1**, calculated at the B3LYP/cc-pVDZ level of theory.

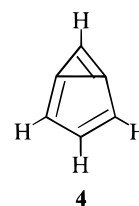
and triplet **1** at the B3LYP/cc-pVDZ level of theory by Nash and Squires.³⁹ The calculations predict that photodetachment should give rise to a total of four active vibrational modes, with unscaled frequencies of 583, 1328, 1427, and 1622 cm^{-1} . The normal coordinate displacement vectors for each of these modes are illustrated in Figure 7. As noted previously, the lowest frequency mode is similar to ν_{6a} in benzene. The 1328 cm^{-1} mode is best described as a “bond alternation” type vibration (a “Kekule mode”) of triplet **1**. The two higher frequencies correspond to ring deformations.

The calculated vibrational frequencies cannot be considered sufficiently accurate to be assigned directly to those observed in the photoelectron spectrum. However, we can use the results for the deuterated ion to aid in the remaining assignments. In the spectrum of **1d**⁻, we find vibrational frequencies of 1265 ± 40 and 1515 ± 40 cm^{-1} . The mode with $\nu = 1395$ cm^{-1} in undeuterated **1** becomes nearly degenerate with the mode corresponding to $\nu = 1265$ cm^{-1} in **1d**. This suggests that the 1395 cm^{-1} mode contains some contributions from hydrogen motion, while the 1275 and 1520 cm^{-1} modes are essentially unaffected by deuterium substitution. Of the vibrational modes depicted in Figure 7, the one with $\nu = 1427$ cm^{-1} appears to have the largest component of H-atom motion, suggesting that this is the observed mode with $\nu = 1395$ cm^{-1} . This assignment is supported by the DFT calculations, which predict that the frequency of the mode with $\nu = 1427$ cm^{-1} mode should shift to 1342 cm^{-1} upon deuteration, while the frequencies of the modes with $\nu = 1328$ and $\nu = 1622$ cm^{-1} are lowered by only 21 and 26 cm^{-1} , respectively, resulting in frequencies of 1307 and 1596 cm^{-1} . Thus, the frequencies of the two lower frequency modes, 1307 and 1342 cm^{-1} , differ by only 35 cm^{-1} and would not be resolved in our photoelectron spectrum. The vibrational frequencies assigned for the vibrational modes in triplet *o*-benzynes are in good agreement with what is obtained by scaling the B3LYP frequencies by 0.96.

***m*-Benzynes.** For triplet **2**, we observe a single vibrational progression with a frequency of 970 cm^{-1} . The calculated structures for **2**⁻ and triplet **2** obtained at the B3LYP/cc-pVDZ level of theory by Nash and Squires³⁹ indicate a significant difference in the distance between the two dehydrocarbons (C1 and C3), 2.432 Å for **2**⁻ and 2.340 Å for triplet **2**. Therefore, the vibrational activity observed in this region of the spectrum

most likely corresponds to the stretching of the C1–C3 distance (or, correspondingly, C1–C2–C3 angle bending). Molecular orbital⁴⁶ and DFT³⁹ calculations support this assignment. Two symmetric (a_1) modes that involve significant C1–C3 stretching are evident in the DFT calculations for triplet **2**, with (unscaled) frequencies of 610 and 964 cm^{-1} . The lower frequency mode involves significant in-phase C4–C6 stretching, making it similar to the ν_{6a} mode in benzene, while in the higher frequency mode the C1–C3 and C2–C4 stretchings are out of phase and the motion is somewhat more localized in the C1–C3 stretch. The frequency computed for this latter mode matches well with the experimentally determined frequency. The measured vibrational frequency for triplet **2d**, 955 cm^{-1} , is only slightly lower than that for the nondeuterated species, which is consistent with a mode involving mainly the carbon skeleton.

The vibrational structure in the singlet feature for *m*-benzynes is considerably more complex than that in the triplet state. For the singlet state, we observe an extended progression with irregular peak spacings of ca. 300 cm^{-1} , which we have not been able to reproduce using standard harmonic or Morse potentials. This type of vibrational structure could be the result of many different factors. An appealing possibility is that, as with the triplet state, the vibrational structure is mainly due to a single mode involving stretching of the 1,3-distance between the dehydrocarbons. However, in order for this to result in such an extensive vibrational progression, the geometry difference between the ion and the neutral would have to be substantial, and the C1–C3 stretching mode should correspond to a vibrational frequency around 300 cm^{-1} . The geometries and frequencies obtained from ab initio calculations for **2**⁻ and the singlet state of **2** provide only limited guidance. At the MCSCF/3-21G level of theory, the distances between the dehydrocarbons in the ion (²B₂), the neutral triplet (³B₂), and the neutral singlet (¹A₁) are calculated to be 2.436,³⁹ 2.354,⁴⁶ and 2.251 Å,⁴⁶ respectively. While the difference in C1–C3 distance between the ion and the singlet is slightly greater than that between the ion and the triplet, attempts at fitting the singlet region of the spectrum with the MCSCF/3-21G data indicate that the C1–C3 distance is too large to account satisfactorily for the observed shape of the vibrational band. At the other extreme is the “bicyclic” structure **4** computed for singlet *m*-benzynes at the RHF/6-31G(d)⁶³ and B3LYP^{40,65} levels of theory. With these



methods the C1–C3 distances are calculated to be only 1.48 Å (RHF) and 1.62 Å (B3LYP). Optimization to a closed-shell, bicyclic structure for singlet **2** is the expected result from restricted, single-configuration calculations such as these, because the biradical character of the molecule is either completely ignored (RHF) or inadequately represented (B3LYP). Calculations on singlet **2** with “pure” DFT methods such as BLYP and BPW91⁴⁰ that do not include the Hartree–Fock exchange component like B3LYP give somewhat more open structures, with optimized C1–C3 distances of 1.9–2.0 Å. However, as with the MCSCF/3-21G results, the DFT parameters also fail to give an acceptable fit of the singlet region of

(65) Kraka, E.; Cremer, D.; Bucher, G.; Wandel, H.; Sander, W. *Chem. Phys. Lett.* **1997**, *268*, 313.

the *m*-benzyne spectrum, as the computed geometry difference between the ion and neutral is too large.

What, then, can we say about the structure of singlet *m*-benzyne? From the appearance of the spectrum, it is clear that the geometry of the singlet state differs significantly from that of both the ion and the triplet state. The weak bonding interaction between the dehydrocarbons in singlet **2** is evident from theoretical treatments that properly include the multiconfigurational character of this molecule,^{46,63} but even so, simple MCSCF approaches apparently underestimate the effect of this interaction on the geometry. A pure bicyclic form with a short C1–C3 bond such as **4** is ruled out by our inability to fit the spectrum with such a structure. Moreover, the MCSCF and CI energies of bicyclic structures derived from RHF/6-31G(d) calculations are found to be 11–15 kcal/mol higher than the energies of the biradical forms.^{46,63} The CCSD(T)/6-31G(d,p) calculations reported by Kraka and Cremer⁶⁶ and by Marquardt et al.³⁷ probably provide the best model for the structure of singlet *m*-benzyne. This method, which includes estimates for the effects of both static and dynamic electron correlation, gives a structure with a C1–C3 distance of 2.11 Å and an unscaled frequency for the C1–C3 stretching mode of 386 cm⁻¹. Furthermore, Cramer, Nash, and Squires obtained a value for $\Delta E_{\text{ST}}(\mathbf{2})$ at the CCSD(T)/cc-pVTZ level of theory of 20.7 kcal/mol, in excellent agreement with the experimental S–T splitting.⁴⁰ Analysis of the CCSD(T)/6-31G(d,p) wave functions for singlet **2** indicates 20% biradical character.⁶⁵ Therefore, **2** is best described as being intermediate between a pure biradical and a pure bicyclic molecule.

The spectroscopic information obtained for singlet *m*-benzyne from this work complements the low-temperature matrix IR results reported by Marquardt et al.³⁷ The most intense peak in the IR spectrum is observed at 547 cm⁻¹ and assigned to a b₁ ring deformation mode of *m*-benzyne. Several weaker absorptions are observed in the 750–1500 cm⁻¹ range, assigned to CH wagging modes and to skeletal modes involving CC stretching and HCC deformation. No vibrational frequencies below 500 cm⁻¹ are observed in the matrix IR spectrum of *m*-benzyne that might be attributed to C1–C3 stretching.

***p*-Benzyne.** The singlet and triplet bands in the *p*-benzyne ion spectrum exhibit similar vibrational structure. In both cases, the main progression corresponds to a frequency of ca. 600 cm⁻¹, which is believed to result from the same type of symmetric ring deformation mode that is active in the spectrum of **1**⁻ and phenyl anion.⁶¹ The other active mode in both bands has a frequency near 1000 cm⁻¹, which is attributed to ring-breathing. The similarity between the singlet and triplet features in the *p*-benzyne ion spectrum clearly contrasts the marked differences between the singlet and triplet features that are evident in both the *o*- and *m*-benzyne ion spectra (Figure 1). The spectral fitting described earlier indicates that the Franck–Condon factors (ΔQ_i) for the ring deformation modes of singlet and triplet *p*-benzyne are large and within a factor of 2 of each other (Table 1). However, in *o*-benzyne the Franck–Condon factors for this mode differ by a factor of 5, as is readily apparent in the spectrum of **1**⁻. Similarly, a large geometry difference between the singlet and triplet states of *m*-benzyne is immediately apparent from the spectrum of **2**⁻. Therefore, unlike what is found for *o*- and *m*-benzyne, the singlet and triplet states of *p*-benzyne have similar structures. This conclusion is supported by MCSCF calculations employing either large (aANO)⁴⁰ or small (3-21G) basis sets,⁴⁶ which predict geometries for the singlet and triplet states of *p*-benzyne that are

Table 3. Measured Heats of Formation for *o*-Benzyne

$\Delta H_{\text{f},298}(\textit{o}\text{-benzyne})^{a,b}$	method	ref
106.5 ± 2.7	PEPICO ^c	19
113.7 ± 5.0	PA bracketing ^d	20
103.4 ± 3.0	EI AP ^e	21
98.4 ± 3.8	PI AP ^f	22
105.2 ± 3.0	I/M reactions ^g	23
107.5 ± 3.0	acidity bracketing ^h	24
105.1 ± 3.2	CID threshold ⁱ	25
109.0 ± 3.0	acidity bracketing ^h	26
105.9 ± 3.3	average	

^a Values in kcal/mol. ^b Calculated using updated auxiliary thermochemical values; see text. ^c Photoelectron/photoionization coincidence measurement of the heat of formation of **1**⁺. ^d From the bracketed proton affinity of **1**. ^e Electron impact appearance energy measurement of the heat of formation of **1**⁺. ^f Photoionization appearance energy measurement of the heat of formation of **1**⁺. ^g From the reactivity of C₆H₅X (X = Br, I) with OH⁻ and RO⁻. ^h From the bracketed gas-phase acidity of phenyl radical. ⁱ Collision-induced dissociation threshold measurements.

essentially the same. That is, the computed distance between the dehydrocarbons in the two states differ by only 0.03 Å, and the other carbon–carbon bond distances are found to be the same within 0.008 Å. Moreover, the calculations are also correct with respect to the relative geometries of the two electronic states, as the singlet has a slightly longer dehydrocarbon bond distance than the triplet and more closely resembles the ion. The reverse situation is true in **1** and **2**, where the triplet states are more like the ions.

Thermochemistry. The electron affinities and singlet–triplet splittings measured in this work can be used to derive important thermochemical quantities for the benzyne, including heats of formation for the triplet states and values for the C–H bond energies of phenyl radical and phenyl anion. The absolute heats of formation of the singlet benzyne have been addressed previously.^{25,67} In particular, the heat of formation of *o*-benzyne has been measured by eight independent experimental methods, with the results listed in Table 3. Some of the values are slightly different from those given in the original papers because they have been recalculated using updated values for the auxiliary thermochemical data. The new data used for these derivations include the ionization potential of phenyl radical (IP(C₆H₅) = 8.05 ± 0.10 eV),⁶⁸ the IP of *o*-benzyne (9.03 ± 0.05 eV),²⁷ and the C–H bond energy of benzene (D₃₀₀(C₆H₅–H) = 113.5 ± 0.5 kcal/mol).⁶⁷ A weighted average of all the values listed in Table 3 gives $\Delta H_{\text{f},298}(\mathbf{1}) = 105.9 \pm 3.3$ kcal/mol. This is somewhat lower than, but is within error of, the values predicted from isodesmic reaction analyses carried out at the CASPT2,⁴⁰ CCSD(T),^{40,66} and G2⁶⁹ levels of theory. The heat of formation of singlet *m*-benzyne **2** has been determined from CID threshold measurements to be 121.9 ± 3.1 kcal/mol,^{25,67} in good accord with the predictions from CCSD(T) calculations.^{40,66} Two independent experimental measurements of $\Delta H_{\text{f},298}(\mathbf{3})$, 137.8 ± 2.9 and 138.0 ± 1.0 kcal/mol,^{25,67,70} are in excellent agreement with one another and are also fully supported by CCSD(T) calculations.⁴⁰ From the heats of formation for the singlet benzyne and the measured singlet–triplet splittings, we obtain heats of formation of 143.3 ± 3.3, 142.9 ± 3.1, and 141.6 ± 2.9 kcal/mol for the triplet states of **1**, **2**, and **3**, respectively,

(67) Davico, G. E.; Bierbaum, V. M.; DePuy, C. H.; Ellison, G. B.; Squires, R. R. *J. Am. Chem. Soc.* **1995**, *117*, 2590.

(68) Berkowitz, J.; Ellison, G. B.; Gutman, D. *J. Phys. Chem.* **1994**, *98*, 2744.

(69) Raghavachari, K.; Stefanov, B. B.; Curtiss, L. A. *J. Chem. Phys.* **1997**, *106*, 6764.

(70) Roth, W. R.; Hopf, H.; Horn, C. *Chem. Ber.* **1994**, *127*, 1765.

(66) Kraka, E.; Cremer, D. *J. Am. Chem. Soc.* **1994**, *116*, 4929.

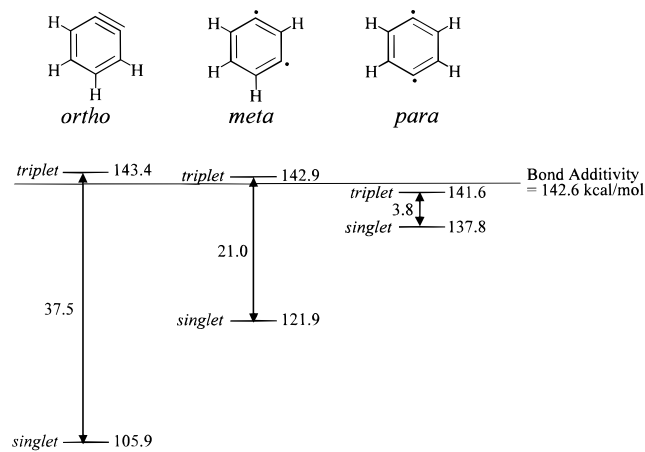


Figure 8. Experimentally determined energies for the singlet and triplet states of **1**, **2**, and **3**. The solid line indicates the simple additivity estimate obtained by assuming the first and second C–H bond strengths of benzene are the same.

where the small (<0.3 kcal/mol) temperature correction for the singlet–triplet splittings have been omitted. The absolute heats of formation for the singlet and triplet states of the benzyne are illustrated in Figure 8. Also shown in Figure 8 is the “bond additivity” estimate for the heat of formation of a didehydrobenzene molecule, 142.6 ± 0.8 kcal/mol, that one derives by assuming that the first and second C–H bond energies of benzene are the same.^{25,67} It is evident that the heats of formation of the triplet states of the benzyne are all the same, within error, as the bond additivity estimate, while the heats of formation of the singlet ground states are essentially equal to the bond additivity estimate minus the singlet–triplet splitting. The unified experimental picture of benzyne thermochemistry illustrated in Figure 8 is consistent with the valence bond (VB) promotion energy model discussed by Chen and co-workers^{27,71} for estimating the energetics of ground-state singlet biradicals.

Absolute heats of formation for the benzyne negative ions, $\Delta H_{f,298}(\text{C}_6\text{H}_6^-)$, can be derived by combining the measured electron affinities and heats of formation for **1**, **2**, and **3**. These are determined to be 92.9 ± 3.3 , 102.3 ± 3.1 , and 108.6 ± 2.9 kcal/mol for **1**[−], **2**[−], and **3**[−], respectively,⁷² in good agreement with the values determined previously from slightly different values of the electron affinities.²⁸ From these quantities we can calculate the gas-phase acidity, ΔH_{acid} , of phenyl radical in the *ortho*, *meta*, and *para* positions. The resulting values, 377.4 ± 3.4 , 386.8 ± 3.2 , and 393.1 ± 3.0 kcal/mol, respectively, are lower than that of benzene, $\Delta H_{\text{acid}}(\text{C}_6\text{H}_6) = 401.7 \pm 0.5$ kcal/mol,⁶⁷ by 8–24 kcal/mol. The substantial increases in the *ortho* and *meta* C–H acidities of phenyl radical originate mainly from the large reduction in the *ortho* and *meta* bond energies compared to benzene,⁶⁷ i.e., they are largely due to biradical stabilizing effects. The smaller increase in acidity of the *para* C–H bond arises in equal amounts from the decreased *para* C–H bond energy and the increased electron binding energy of *p*-benzyne compared to phenyl radical, i.e., the biradical and negative ion stabilization effects are about the same. This same balance of effects is operative in determining the decreased C–H bond energies of phenyl anion compared to benzene. The homolytic bond energies derived from the benzyne anion heats of formation are 89.3 ± 3.3 , 98.7 ± 3.1 , and 105.0 ± 2.9 kcal/mol for the *ortho*-, *meta*-, and *para* positions, respectively.

(71) Clauberger, H.; Minsek, D. W.; Chen, P. *J. Am. Chem. Soc.* **1992**, *114*, 99.

(72) The small temperature correction has been neglected.

Finally, from the thermochemical results measured in this work we can now understand the origins of the *m*-benzyne anion features (but no *p*-benzyne anion features) observed in the photoelectron spectrum of **1**[−]. The reaction of benzene with O^- to form **1**[−], **2**[−], and **3**[−] is determined to have 298 K enthalpy changes of -10 , -2 , and $+5$ kcal/mol, respectively. Therefore, formation of **1**[−] and **2**[−] is thermochemically allowed, while formation of **3**[−] from O^- and benzene is endothermic.

Conclusion

With the singlet–triplet splittings determined in this study, and the heats of formation of the ground states determined previously,²⁵ we now have absolute energies for all of the low-lying states of the isomeric benzyne. The picture that emerges is a remarkable one, which provides valuable insights into the structures and electronic interactions within this class of biradical. The relative stabilities of the singlet ground states, $\Delta H_f(\mathbf{1}) < \Delta H_f(\mathbf{2}) < \Delta H_f(\mathbf{3})$, reflect the extent of electronic interaction between the dehydrocarbons. *o*-Benzyne, **1**, has a strong bonding interaction arising from direct, front-side overlap of the two in-plane orbitals, while the weaker interaction in **2** results from the less effective overlap of the rear lobes of these orbitals. The even smaller interaction in **3** arises from a through-bond coupling effect. The similar energies for the benzyne triplet states reflect the absence of electronic interaction between the dehydrocarbons; these states are best described as biradicals containing two independent phenyl radical moieties. The structural consequences of these interactions are clear. The benzyne triplets will have phenyl radical-like geometries with small deviations to accommodate two phenyl radical sites, while the geometries of the singlets will be distorted in such a manner so to maximize the interaction between the dehydrocarbons. For *o*- and *m*-benzyne, this manifests as a reduction in the dehydrocarbon bond distances to optimize overlap. A short, alkyne-like C1–C2 bond results for *o*-benzyne, while in *m*-benzyne the system distorts toward a bicyclic structure. In singlet *p*-benzyne the geometry distorts to increase the through-bond interaction, resulting in an increased distance between the dehydrocarbons compared to the triplet.

The features observed in the negative ion photoelectron spectra reported here reflect these interactions as well. The *o*- and *m*-benzyne spectra clearly show that the negative ions closely resemble the triplet states, consistent with the expectation that the ions, like the triplets, should have relatively weak interactions between the dehydrocarbons. In contrast, the shapes of the spectral features corresponding to formation of the *o*- and *m*-benzyne singlet states indicate significantly different structures relative to the ions, consistent with the much stronger electronic interactions in the ground states of these biradicals. In the case of *p*-benzyne the spectral features for the singlet and triplet states are similar, indicating that the different electronic interactions in two states do not lead to large differences in their geometries. Moreover, the observed vibrational activity in all three spectra indicate that the main geometry differences between the ion and the neutral are in the normal coordinate corresponding to stretching of the distance between the dehydrocarbons.

Acknowledgment. We thank Joseph Kim and Karl-Ludwig Jonas for assistance with the photoelectron measurements. We especially thank Professor Wolfram Sander for insightful discussion about the IR spectra of *m*- and *p*-benzyne. This work was supported by the National Science Foundation (W.C.L.: CHE97-03486, PHY95-12150 R.R.S.: CHE-9221489).